non-parametric Mann–Whitney *U*-test (for within-syllable changes) and paired sign test (for group changes). Comparisons of variability of fundamental frequency in different experimental conditions were made using the *F*-test for equality of variance. In all cases, the minimum significance level was set at $P < 0.05$.

Received 3 August; accepted 21 October 2004; doi:10.1038/nature03127.

1. Graybiel, A. M., Aosaki, T., Flaherty, A. W. & Kimura, M. The basal ganglia and adaptive motor control. *Science* **265,** 1826–1831 (1994).
2. Bottjer, S. W., Miesner, E. A. & Arnold, A. P. Forebrain lesions disrupt development but not maintenance of song in passerine birds. *Science* **224,** 901–903 (1984).
3. Scharff, C. & Nottebohm, F. A comparative study of the behavioral deficits following lesions of various parts of the zebra finch song system: implications for vocal learning. *J. Neurosci.* **11,** 2896–2913 (1991).
4. Brainard, M. S. & Doupe, A. J. Interruption of a basal ganglia–forebrain circuit prevents plasticity of learned vocalizations. *Nature* **404,** 762–766 (2000).
5. Williams, H. & Mehta, N. Changes in adult zebra finch song require a forebrain nucleus that is not necessary for song production. *J. Neurobiol.* **39,** 14–28 (1999).
6. Tchernichovski, O., Mitra, P. P., Lints, T. & Nottebohm, F. Dynamics of the vocal imitation process: how a zebra finch learns its song. *Science* **291,** 2564–2569 (2001).
7. Williams, H., Cynx, J. & Nottebohm, F. Timbre control in zebra finch (*Taeniopygia guttata*) song syllables. *J. Comp. Psychol.* **103,** 366–380 (1989).
8. Nottebohm, F., Stokes, T. M. & Leonard, C. M. Central control of song in the canary. *J. Comp. Neurol.* **165,** 457–486 (1976).
9. Perkel, D. J. in *Behavioral Neurobiology of Birdsong* (eds Zeigler, H. P. & Marler, P.) 736–748 (New York Academy of Sciences, New York, 2004).
10. Troyer, T. W. & Doupe, A. J. An associational model of birdsong sensorimotor learning. II. Temporal hierarchies and the learning of song sequence. *J. Neurophys.* **84,** 1224–1239 (2000).
11. Doya, K. & Sejnowski, T. J. in *The New Cognitive Neurosciences* (ed. Gazzaniga, M. S.) 469–482 (MIT Press, Cambridge, Massachusetts, 2000).
12. Hessler, N. A. & Doupe, A. J. Social context modulates singing-related neural activity in the songbird forebrain. *Nature Neurosci.* **2,** 209–211 (1999).
13. Hessler, N. A. & Doupe, A. J. Singing-related neural activity in a dorsal forebrain–basal ganglia circuit of adult zebra finches. *J. Neurosci.* **19,** 10461–10481 (1999).
14. Vu, E. T., Mazurek, M. E. & Kuo, Y. C. Identification of a forebrain motor programming network for the learned song of zebra finches. *J. Neurosci.* **14,** 6924–6934 (1994).
15. Vicario, D. S. & Simpson, H. B. Electrical stimulation in forebrain nuclei elicits learned vocal patterns in songbirds. *J. Neurophys.* **73,** 2602–2607 (1995).
16. Brumm, H. & Todt, D. Male–male vocal interactions and the adjustment of song amplitude in a territorial bird. *Anim. Behav.* **67,** 281–286 (2004).
17. Yu, A. C. & Margoliash, D. Temporal hierarchical control of singing in birds. *Science* **273,** 1871–1875 (1996).
18. Johnson, F., Sablan, M. M. & Bottjer, S. W. Topographic organization of a forebrain pathway involved with vocal learning in zebra finches. *J. Comp. Neurol.* **358,** 260–278 (1995).
19. Mooney, R. Different subthreshold mechanisms underlie song selectivity in identified HVc neurons of the zebra finch. *J. Neurosci.* **20,** 5420–5436 (2000).
20. Jarvis, E. D., Scharff, C., Grossman, M. R., Ramos, J. A. & Nottebohm, F. For whom the bird sings: context-dependent gene expression. *Neuron* **21,** 775–788 (1998).
21. Hikosaka, O., Nakamura, K., Sakai, K. & Nakahara, H. Central mechanisms of motor skill learning. *Curr. Opin. Neurobiol.* **12,** 217–222 (2002).
22. Miller, E. K. The prefrontal cortex and cognitive control. *Nature Rev. Neurosci.* **1,** 59–65 (2000).
23. Troyer, T. W. & Bottjer, S. W. Birdsong: models and mechanisms. *Curr. Opin. Neurobiol.* **11,** 721–726 (2001).
24. Mooney, R. & Konishi, M. Two distinct inputs to an avian song nucleus activate different glutamate receptor subtypes on individual neurons. *Proc. Natl Acad. Sci. USA* **88,** 4075–4079 (1991).
25. Kittelberger, J. M. & Mooney, R. Lesions of an avian forebrain nucleus that disrupt song development alter synaptic connectivity and transmission in the vocal premotor pathway. *J. Neurosci.* **19,** 9385–9398 (1999).
26. Stark, L. L. & Perkel, D. J. Two-stage input-specific synaptic maturation in a nucleus essential for vocal production in the zebra finch. *J. Neurosci.* **19,** 9107–9116 (1999).
27. Komatsu, H. & Wurtz, R. H. Modulation of pursuit eye movements by stimulation of cortical areas MT and MST. *J. Neurophys.* **62,** 31–47 (1989).
28. Tanaka, M. & Lisberger, S. G. Regulation of the gain of visually guided smooth-pursuit eye movements by frontal cortex. *Nature* **409,** 191–194 (2001).
29. Canales, J. J. & Graybiel, A. M. A measure of striatal function predicts motor stereotypy. *Nature Neurosci.* **3,** 377–383 (2000).
30. Matsumoto, N., Hanakawa, T., Maki, S., Graybiel, A. M. & Kimura, M. Nigrostriatal dopamine system in learning to perform sequential motor tasks in a predictive manner. *J. Neurophys.* **82,** 978–997 (1999).

Supplementary Information accompanies the paper on **www.nature.com/nature**.

Acknowledgements We thank N. Hessler for a portion of the data in Fig. 3e. We thank A. Basbaum, S. Lisberger, J. Sakata and B. Wright for helpful comments on this manuscript and A. Arteseros and K. McManaway for technical assistance. This work was supported by an HHMI Predoctoral Fellowship (M.H.K.), the MacArthur Foundation, the Steven and Michele Kirsch Foundation, NARSAD and NIH (A.J.D.), and the HHMI Biomedical Research Support Program grant, the McKnight Foundation, the Klingenstein Fund, a Searle Scholars Award and NIH (M.S.B.).

Competing interests statement The authors declare that they have no competing financial interests.

Correspondence and requests for materials should be addressed to M.H.K. (mimi@phy.ucsf.edu).

Ultrabithorax is required for membranous wing identity in the beetle *Tribolium castaneum*

Yoshinori Tomoyasu[1], Scott R. Wheeler[2]* & Robin E. Denell[1]

[1]*Division of Biology, Chalmers Hall, Kansas State University, Manhattan, Kansas 66506, USA*
[2]*Department of Genetics, Washington University School of Medicine, 4566 Scott Avenue, St Louis, Missouri 63110, USA*

* Present address: Program in Molecular Biology and Biotechnology, The University of North Carolina at Chapel Hill, Campus Box 3280 - Fordham Hall, Chapel Hill, North Carolina 27599-3280, USA

The two pairs of wings that are characteristic of ancestral pterygotes (winged insects) have often undergone evolutionary modification. In the fruitfly, *Drosophila melanogaster*, differences between the membranous forewings and the modified hindwings (halteres) depend on the Hox gene *Ultrabithorax* (*Ubx*). The *Drosophila* forewings develop without Hox input, while *Ubx* represses genes that are important for wing development, promoting haltere identity[1,2]. However, the idea that Hox input is important to the morphologically specialized wing derivatives such as halteres, and not the more ancestral wings, requires examination in other insect orders. In beetles, such as *Tribolium castaneum*, it is the forewings that are modified (to form elytra), while the hindwings retain a morphologically more ancestral identity. Here we show that in this beetle *Ubx* 'de-specializes' the hindwings, which are transformed to elytra when the gene is knocked down. We also show evidence that elytra result from a Hox-free state, despite their diverged morphology. *Ubx* function in the hindwing seems necessary for a change in the expression of *spalt*, *iroquois* and *achaete-scute* homologues from elytron-like to more typical wing-like patterns. This counteracting effect of *Ubx* in beetle hindwings represents a previously unknown mode of wing diversification in insects.

Many modern insects have wings on their second (T2) and third (T3) thoracic segments. Wing morphology often differs greatly between species, and sometimes between forewing and hindwing in the same species. In *Drosophila*, the forewing is used for flight, while the hindwing (haltere) is highly reduced and used only for balance (Fig. 1a). *Ubx* promotes haltere identity by repressing expression of some wing genes, including those of the *spalt* (*sal*) complex[2] (Fig. 1a), but not others such as *optomotor blind* (*omb*; *bifid*, *bi* in Flybase)[2]. Removing *Ubx* function causes the transformation of haltere to forewing[1] (typically referred to simply as 'wing'). In contrast, the forewing is thought to be a Hox-free state, because inactivating or overexpressing *Antennapedia* (*Antp*), the only Hox gene expressed in the forewing, has almost no effect on wing morphology[3,4]. No wings develop on T1 or the abdominal segments, because *Sex combs reduced* (*Scr*), *Ubx* and *abdominal-A* (*abd-A*) repress wing development in these segments[3] (Fig. 1a). Despite the divergence of hindwing morphology between dipterans (flies) and lepidopterans (butterflies and moths), *Ubx* also regulates hindwing identity in the butterfly *Precis coenia*, albeit by regulating a different set of target genes than those in *Drosophila*[5,6]. Weatherbee *et al.*[5] proposed that diversification of wing morphology among insects was achieved both by modification of a basic wing-gene network that controls both fore- and hindwing development in a species-specific and *Ubx*-independent manner, and by the divergence of *Ubx*-regulated target genes (rather than by changes in *Ubx* expression) in the hindwing.

Applying these models to beetle wing development is confusing, as the situation in beetles is the opposite to that in *Drosophila*: the T2 segment bears sclerotized elytra (wing covers) (Fig. 1b, c), whereas

the T3 segment develops more typical membranous flight wings (hereafter referred to as 'hindwings') (Fig. 1e). One possible explanation is that *Ubx* is expressed differently in beetles. However, detection of Ultrathorax (Utx), the protein product of the *Tribolium Ubx* orthologue, by monoclonal antibody FP6.86 (ref. 7) shows that Utx, like its *Drosophila* counterpart, is expressed in T3 but not in T2 imaginal discs (Fig. 1f, g). This indicates that the function of *Ubx* and/or other Hox genes could be different in beetles.

To examine the function of Hox genes in beetle wing differentiation, we analysed the adult phenotypes of Hox gene mutants in *Tribolium*. Loss-of-function mutants of *Cephalothorax* (*Cx*), the *Tribolium* counterpart of *Scr* (ref. 8), have additional elytron-like tissue on the pronotum (T1)[9,10] (Fig. 1h), suggesting that *Scr*/*Cx* function in repressing T1 wing development is conserved between fly and beetle. *Scr*/*Cx* does not seem to have any further effect on wing development, as elytron and hindwing morphology is normal in these mutants (data not shown). Mutation of the *Antp* orthologue, *prothoraxless* (*ptl*)[10–12], causes reduction of the pronotum[10] (Fig. 1i) but has no visible effect on hindwings (data not shown) or elytra (Fig. 1i). However, it is unclear whether the pronotum phenotype results from loss- or gain-of-function. The situation is similar for *Ubx*/*Utx* mutants, as some mutants (for example, *Utx*[1]) that have a loss-of-function phenotype in embryogenesis, seem to have a gain-of-function phenotype affecting elytra at the adult stage[13].

To determine the Hox gene functions during wing differentiation more clearly in this beetle, we have established a larval RNA interference (RNAi) technique to knock down gene function during imaginal development[14] (see Methods). An enhancer-trap line (*pu11*), which expresses green fluorescent protein (GFP) in hindwing and elytron discs[15] (Fig. 2a, f), was used to visualize hindwing and elytron development in larvae. Injection of *Scr*/*Cx* double-stranded (ds)RNA at a late larval stage (sixth to eighth instar) induces additional GFP-positive tissues in the T1 segment of larvae (Fig. 2b) and ectopic elytra on the pupal and adult pronotum (Fig. 2d; Supplementary Fig. 1). This phenotype is consistent with that of existing *Cx* mutants (Fig. 1h), indicating that RNAi is working properly in beetle larvae and pupae. We then used larval RNAi to determine the function of *Ubx*/*Utx* during hindwing/elytron development. *Ubx*/*Utx* RNAi induced complete transformation of hindwing to elytron (Fig. 2c, e). The transformed elytra

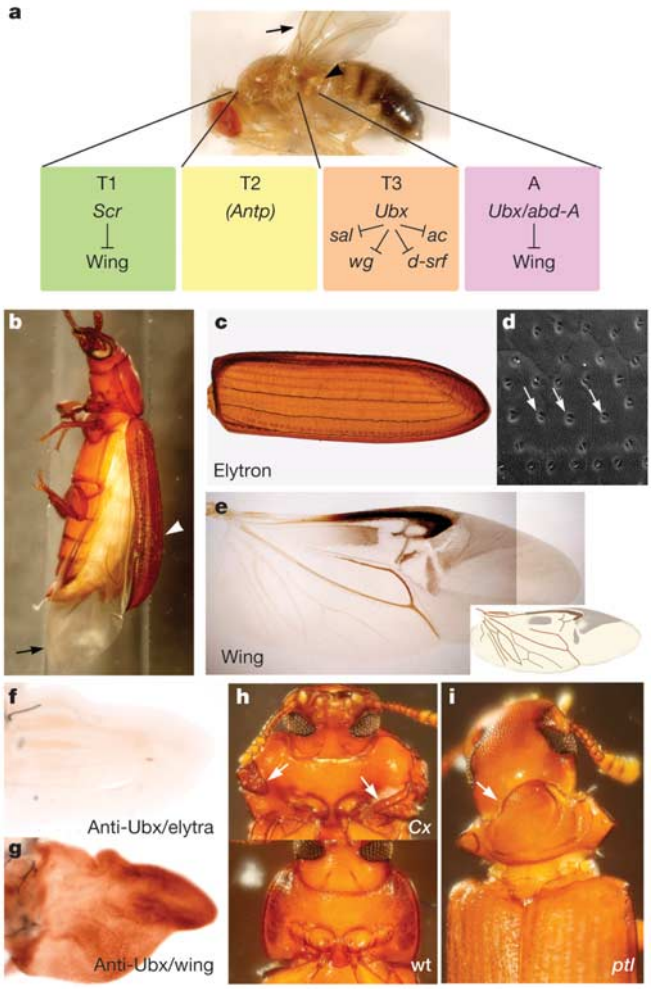

Figure 1 Function of Hox genes in fore- and hindwing differentiation in insects. **a**, A model for fore- and hindwing differentiation in *Drosophila*. Wing (arrow) and haltere (arrowhead) are indicated. *wg*, *wingless*; *d-srf*, *Drosophila serum response factor*. Adult (**b**), elytron (arrowhead in **b**, **c**) and its scanning electron microscopy image (**d**), and hindwing (arrow in **b**, **e**) of *Tribolium castaneum*. Elytra are covered by numerous sensory bristles (**d**, indicated by arrows). **f**, **g**, Ubx/Utx expression in elytra (**f**) and hindwing disc (**g**) monitored by FP6.86. **h**, Ventral view of Cx^{6}/Cx^{apt}. Ectopic tissue on the pronotum is indicated by arrows. Bottom: wild type. **i**, ptl^{D60}/ptl^{D2}. Arrow indicates the reduced pronotum.

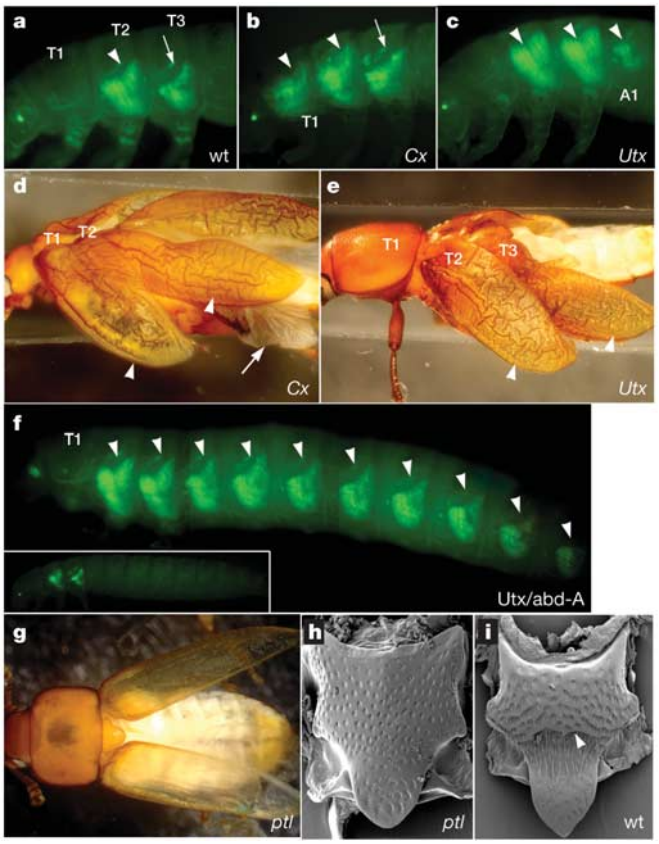

Figure 2 RNAi phenotypes of Hox genes in *Tribolium*. Elytron and wing are denoted by arrowheads and arrows, respectively. **a**, *pu11* larva. GFP is expressed in elytron and hindwing discs. *Scr*/*Cx* RNAi induces ectopic elytra in the T1 segment (**b**, **d**). *Ubx*/*Utx* RNAi larva (**c**) and adult (**e**). Hindwings are transformed into elytra (**c**, **e**). A1 has ectopic GFP-expressing tissue (**c**). **f**, *Ubx*/*Utx* and *abd-A*/*A* double RNAi larva, which has 20 elytron discs from T2 to A8. Inset shows full-length of *pu11* larva. *Antp*/*ptl* RNAi adult (**g**) and mesonotum (**h**). The scutoscutellar ridge (arrowhead in **i**) is missing and bristle pattern is uniform in *Antp*/*ptl* RNAi mesonotum (**h**, compare with **i**, wild type). Anterior is to the left in all images, except for the scanning electron microscopy images (**h**, **i**) in which anterior is up.

often appear almost transparent because *Ubx*/*Utx* RNAi beetles die before the elytra are sclerotized and pigmented. However, their morphology (for example, sensory structures and vein patterning) is clearly specific to the elytra (Supplementary Fig. 1). *Ubx*/*Utx* RNAi also affects the first abdominal (A1) segment, inducing small ectopic GFP-expressing regions in larvae (Fig. 2c) and cylindrical projections in adults (Supplementary Fig. 2a), which presumably represent incompletely developed elytra. In addition, dorsal structures of the T3 and A1 segments are transformed to T2 mesonotum (Supplementary Fig. 2a). Double RNAi using *Ubx*/*Utx* and *Abdominal* (*A*), the *abd-A* orthologue, also induces transformation of the hindwing discs to elytra, accompanied by the development of presumptive elytra in all larval abdominal segments (Fig. 2f); these larvae did not survive to the pupal stage. These phenotypes parallel the results in *Drosophila* with respect to the segments affected, but are unexpected on the basis of the regulatory paradigm indicated by *Drosophila* studies. Unlike *Drosophila Ubx*, which normally modifies membranous wing development to produce halteres, *Ubx*/*Utx* in this beetle seems to promote membranous hindwing development by repressing elytron identity.

In contrast to the marked phenotypes of *Ubx*/*Utx* and *abd-A*/*A* RNAi, *Antp*/*ptl* RNAi induces a rather mild adult phenotype. Several furrow structures (or sutures) on the mesonotum (the median ridge and scutoscutellar ridge[16]) are missing and the microchaete pattern on this structure is more uniform than in the wild type (Fig. 2g, h; compare with Fig. 2i; see Supplementary Fig. 2b, c). However, there is no identifiable effect on the hindwings or elytra (Fig. 2g). These observations indicate that *Antp*/*ptl* has no obvious function in wing differentiation. These data therefore indicate that the elytra represent a Hox-free state, despite their derived morphology, and that *Ubx*/*Utx* promotes membranous wing identity in the hindwing of beetles.

To understand how *Ubx*/*Utx* regulates hindwing development, we analysed the expression patterns of more than 15 wing genes in *Tribolium* hindwing and elytron imaginal discs. Most genes are expressed similarly in elytron and hindwing (Y.T., manuscript in preparation). However, *Tribolium* homologues of *sal*, *iroquois* (*iro*) complex genes and *achaete-scute* (*ac-sc*) are expressed differently in T2 versus T3 imaginal discs (Fig. 3). In the *Drosophila* wing disc, *sal* is induced by Decapentaplegic (Dpp) signalling along the anterior/posterior compartment boundary[17]. A *Tribolium sal* homologue (*Tc-sal*) is expressed in the distal part of the hindwing disc during the last larval stage (Fig. 3f). However, the only *Tc-sal* expression in the elytron disc is faint posterior marginal expression (Fig. 3b inset). In contrast, *Tc-dpp* (ref. 18) and *Tc-omb* (a homologue of another gene regulated by Dpp in *Drosophila*)[19], are expressed similarly in both the hindwing and elytron discs (Fig. 3a, e; data not shown). *Tc-iro* is expressed in two short stripes in the hindwing disc of *Tribolium* (Fig. 3g). Double staining with an antibody against Engrailed (Supplementary Fig. 3) suggests that these stripes correspond to *iro* expression in the L3 and L5 veins of the *Drosophila* wing disc[20]. In the elytron disc, *Tc-iro* is expressed in sensory organ precursor cells, but no stripe expression is observed (Fig. 3c). We also noticed that the *Tc-ac-sc-homologue* (*Tc-ASH*)[21] is expressed in stripes across the entire elytron disc (Fig. 3d), but only a few *Tc-ASH*-positive regions are seen in hindwing discs (Fig. 3h). *ac-sc* is known to be important for sensory organ development[22], and the observed expression is consistent with the sensory organ pattern of these structures. The *Tc-sal* expression at the posterior margin of the elytron disc (Fig. 3c) is interesting as this region corresponds to the anal marginal area for articulation[16], a less sclerotized band of tissue in adult elytra. *Tc-sal* expression might be important for preventing sclerotization in beetle elytron and hindwing. It is also intriguing that both *iro* and *sal* are important for vein positioning in the *Drosophila* wing disc[17,20,23,24]. Modification of the gene network for wing vein formation might be important for hindwing/elytron

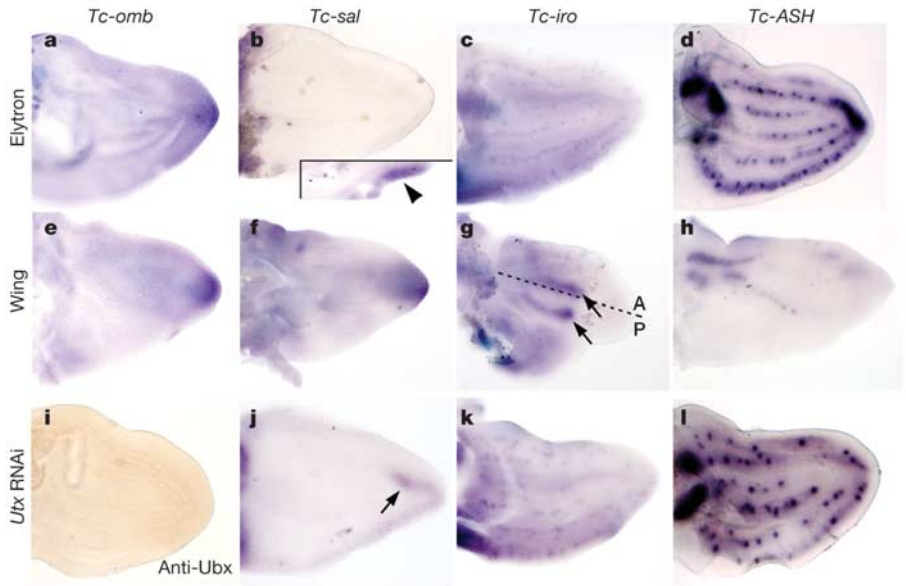

Figure 3 Wing genes' expression in hindwing and elytron disc. *Tc-omb* is expressed similarly in both elytron and hindwing discs (**a**, **e**), however, *Tc-sal* expression is absent in the elytron disc (**b**, **f**), except for faint expression along the posterior margin, which can be seen after longer staining reaction (arrowhead in inset in **b**). Two stripes of *Tc-iro* expression are observed in hindwing (arrows in **g**), but not elytron discs (**c**). Dashed line indicates the anterior/posterior border. *Tc-iro* is expressed in sensory organ precursor cells in elytra (**c**). *Tc-ASH* expression is detected in several stripes in elytron discs (**d**), but is largely absent in hindwing discs (**h**). Ubx/Utx (**i**), *Tc-sal* (**j**), *Tc-iro* (**k**) and *Tc-ASH* (**l**) expression in *Ubx*/*Utx* RNAi hindwings. Ubx/Utx is not detected by FP6.86, indicating that RNAi is working properly (**i**). Distal expression of *Tc-sal* and two *Tc-iro* stripes are missing in these discs (**j**, **k**). Residual *Tc-sal* expression is sometimes observed (arrow in **j**). *Tc-ASH* is ectopically expressed in *Ubx*/*Utx* RNAi discs, although the stripes are sometimes disoriented (**l**). These expression patterns in *Ubx*/*Utx* RNAi hindwing discs are more similar to those in elytron discs. Discs are shown with anterior up and distal to the right.

differentiation. To determine whether *Ubx*/*Utx* regulates the expression of these genes, we analysed the expression of *Tc-sal*, *Tc-iro* and *Tc-ASH* in *Ubx*/*Utx* RNAi hindwing discs, and found that expression of all three genes is altered. *Tc-sal* distal expression is greatly reduced (sometimes completely missing) and faint posterior margin expression is observed instead (Fig. 3j). The two stripes of *Tc-iro* expression are missing (Fig. 3k), and *Tc-ASH* is ectopically expressed (Fig. 3l). These results indicate that *Ubx*/*Utx* promotes membranous hindwing identity in part by controlling the expression of these genes in *Tribolium*.

It has been proposed that the dorsal appendages of insects first appeared under no (or lesser) Hox influence[3]. Eventually, some Hox genes gained influence over the wing-gene network, probably via alterations in the *cis*-regulatory elements of these genes[3]. *Ubx* is expressed in the hindwings of all insects so far examined[2,6,25]—Diptera, Lepidoptera, Hymenoptera (ants, bees, wasps) and Coleoptera (beetles)—and modifies their structure to varying degrees. Modification of the wing programme by *Ubx* in Lepidoptera and Hymenoptera, as inferred from morphology, seems to be rather minor, resulting in a hindwing structure similar to forewings. In Diptera, the modification by *Ubx* is more extreme and produces the haltere. Our data demonstrate that in beetles, the wing programme has been significantly altered into an 'elytron programme', and that *Ubx*/*Utx* represses at least some of these changes, resulting in a more ancestral morphology. That is, *Ubx*/*Utx* has become indispensable for membranous wing differentiation in the beetle lineage, whereas in other insects, membranous wings can develop with or without *Ubx* expression. It could be argued that the elytra are ancestral (on the basis of their location on T2) and that the beetle hindwing is derived. However, our data show that the gene expression patterns of beetle hindwings are more similar to those of fly forewings than are those of the elytra, indicating that the beetle hindwing represents the more ancestral state. This is further supported by the expression pattern of a *sal* homologue in a Hymenopteran insect[25]. In this case, *sal* expression in both wings resembles that seen in beetle hindwings. Further genetic analysis of beetles as well as other insect orders is necessary to resolve this issue.

There are several possible scenarios to explain the evolution of an 'elytron programme' and the counteracting function of *Ubx*/*Utx* in beetles. One explanation is that the wing programme has recruited several elytron genes (such as cuticle thickening genes), and that *Ubx*/*Utx* represses these genes in hindwings. This might explain the textural modification and other morphological changes of the elytra, although it may be necessary to consider several more scenarios to explain the morphology of this highly specialized appendage. For instance, one or more non-Hox genes (referred to as gene(s) X) could have come to control the expression of wing genes such as *Tc-sal*, *Tc-iro* and *Tc-ASH* in a way that promotes elytron identity. *Ubx*/*Utx* would then suppress the functions of gene(s) X to prevent elytron differentiation in the hindwing. Alternatively, *Ubx*/*Utx* may have become integrated into the wing-gene network. That is, some genes in the wing network might have acquired Ubx/Utx binding sites in their *cis*-regulatory regions, such that this network was no longer able to induce typical membranous wing in the absence of Ubx/Utx. Another possibility is that characteristics of the Utx protein itself (such as binding affinity) might have been altered such that Utx now regulates genes in the wing-gene network. It is possible that a combination of these scenarios accounts for the unusual function of Utx in beetles. Finally, although beetle hindwings seem to be less derived than the elytra, it is obvious that the beetle hindwing has also been evolutionarily modified. Thus, *Ubx*/*Utx* might also modify hindwing in a manner similar to its function in *Drosophila* and other insects[2]. Identification of gene(s) X and analyses of *cis*-elements for the genes that are expressed differently in elytron and hindwing will be necessary for a detailed understanding of *Ubx* function in beetle hindwing, as well as insight into the general mechanisms regulating fore- and hindwing differentiation in all winged insects. □

Methods

Beetles

All beetle strains were raised at 30 °C. The following mutants and transgenic beetles were used in this study. Cx^6 and Cx^{apt} are *Cx* loss-of-function mutants[9,10]. Cx^{apt} is a weak *Cx* hypomorphic allele, while Cx^6 is a null allele that encodes a truncated version of the Cx protein (Rogers and Denell, unpublished data). ptl^{D2} and ptl^{D60} seem to behave as loss-of-function alleles in the embryonic stage[26]. The *pu11* enhancer-trap line[15], previously referred to as Pig-23 (ref. 15), was also used for visualizing hindwing and elytron development in the larval stage.

Cloning genes

Fragments of beetle genes were obtained by polymerase chain reaction (PCR) with reverse transcription using degenerate primers targeted to the motifs conserved between fly and human. Extra fragments were also obtained by universal PCR[27]. The motifs targeted in each protein are as follows. Sal: MHYRTHTGERPFKC (for two nested primers) and VLQQHIR. Iro: KNPYPTKGEKI and ANARRRLKKENKMTW (for two nested primers). Omb: GTEMVITKSGR, YKFHNSRWMVAGKAD and TQLKIDNNPFAKG.

Dissection and staining

In *Tribolium*, hindwing and elytron imaginal discs develop during the last larval stage, in a fashion similar to the mealworm beetle[28] (Y.T., manuscript in preparation). Crude dissections of larval discs were performed in phosphate-buffered saline (PBS). These large tissue fragments containing imaginal discs were then pre-fixed in 3.7% formaldehyde/PBS for 5 min. After the removal of unnecessary tissues in PBS, imaginal discs were fixed in 3.7% formaldehyde/PBS for 30 min. Antibody staining was performed by standard procedures. Monoclonal antibody FP6.86 (1:5, gift from R. White), which recognizes an evolutionarily conserved epitope common to both Ubx and abd-A[7], was used to monitor Ubx/Utx expression, and anti-mouse IgG conjugated to horseradish peroxidase (1:200, Jackson) was used as the secondary antibody. The 4D9 anti-Engrailed antibody developed by C. Goodman was obtained from the Developmental Studies Hybridoma Bank (DSHB) (developed under the auspices of the NICHD and maintained by The University of Iowa, Department of Biological Sciences). *In situ* hybridization was performed using standard procedures.

dsRNA synthesis and injection

dsRNA was synthesized using the Ambion MEGAscript high yield transcription kit. The sizes of dsRNA used in this work are as follows. Cx: 930 bp; ptl: 538 bp; Utx: 450 bp; abd-A: 621 bp. We injected 0.4–0.5 μg of dsRNA into last (or penultimate) instar *pu11* larvae just before the onset of GFP expression in the hindwing and elytron disc (selected by GFP expression), and demonstrated that RNAi works even in the larval stage of *Tribolium* (larval RNAi)[14]. Injected larvae were kept at 30 °C until the proper stage for analysis.

Image processing

Some images were processed using Auto-Montage (Syncroscopy), and brightness and contrast of all images were adjusted with Photoshop (Adobe).

Received 12 October; accepted 13 December 2004; doi:10.1038/nature03272.

1. Lewis, E. B. A gene complex controlling segmentation in *Drosophila*. *Nature* **276,** 565–570 (1978).
2. Weatherbee, S. D., Halder, G., Kim, J., Hudson, A. & Carroll, S. Ultrabithorax regulates genes at several levels of the wing-patterning hierarchy to shape the development of the *Drosophila* haltere. *Genes Dev.* **12,** 1474–1482 (1998).
3. Carroll, S. B., Weatherbee, S. D. & Langeland, J. A. Homeotic genes and the regulation and evolution of insect wing number. *Nature* **375,** 58–61 (1995).
4. Struhl, G. Genes controlling segmental specification in the *Drosophila* thorax. *Proc. Natl Acad. Sci. USA* **79,** 7380–7384 (1982).
5. Weatherbee, S. D. *et al.* *Ultrabithorax* function in butterfly wings and the evolution of insect wing patterns. *Curr. Biol.* **9,** 109–115 (1999).
6. Warren, R. W., Nagy, L., Selegue, J., Gates, J. & Carroll, S. Evolution of homeotic gene regulation and function in flies and butterflies. *Nature* **372,** 458–461 (1994).
7. Kelsh, R., Weinzierl, R. O., White, R. A. & Akam, M. Homeotic gene expression in the locust *Schistocerca*: an antibody that detects conserved epitopes in Ultrabithorax and abdominal-A proteins. *Dev. Genet.* **15,** 19–31 (1994).
8. Curtis, C. D. *et al.* Molecular characterization of *Cephalothorax*, the *Tribolium* ortholog of *Sex combs reduced*. *Genesis* **30,** 12–20 (2001).
9. Beeman, R. W. A homeotic gene cluster in the red flour beetle. *Nature* **327,** 247–249 (1987).
10. Beeman, R. W., Stuart, J. J., Haas, M. S. & Denell, R. E. Genetic analysis of the homeotic gene complex (HOM-C) in the beetle *Tribolium castaneum*. *Dev. Biol.* **133,** 196–209 (1989).
11. Brown, S. J. *et al.* Sequence of the *Tribolium castaneum* homeotic complex: the region corresponding to the *Drosophila melanogaster* Antennapedia complex. *Genetics* **160,** 1067–1074 (2002).
12. Stuart, J. J., Brown, S. J., Beeman, R. W. & Denell, R. E. A deficiency of the homeotic complex of the beetle *Tribolium*. *Nature* **350,** 72–74 (1991).
13. Bennett, R. L., Brown, S. J. & Denell, R. E. Molecular and genetic analysis of the *Tribolium Ultrabithorax* ortholog, *Ultrathorax*. *Dev. Genes Evol.* **209,** 608–619 (1999).
14. Tomoyasu, Y. & Denell, R. E. Larval RNAi in *Tribolium* (Coleoptera) for analyzing adult development. *Dev. Genes Evol.* **214,** 575–578 (2004).
15. Lorenzen, M. D. *et al.* *piggyBac*-mediated germline transformation in the beetle *Tribolium castaneum*.

Insect Mol. Biol. **12,** 433–440 (2003).
16. El-Kifl, A. H. Morphology of the adult *Tribolium confusum* Duv. and its differentiation from *Tribolium* (*stene*) *castaneum* Herbst. *Bull. Soc. Fouad 1er Entom.* **37,** 173–249 (1953).
17. de Celis, J. F., Barrio, R. & Kafatos, F. C. A gene complex acting downstream of *dpp* in *Drosophila* wing morphogenesis. *Nature* **381,** 421–424 (1996).
18. Sanchez-Salazar, J. *et al.* The *Tribolium decapentaplegic* gene is similar in sequence, structure, and expression to the *Drosophila dpp* gene. *Dev. Genes Evol.* **206,** 237–246 (1996).
19. Grimm, S. & Pflugfelder, G. O. Control of the gene *optomotor-blind* in *Drosophila* wing development by *decapentaplegic* and *wingless*. *Science* **271,** 1601–1604 (1996).
20. Gomez-Skarmeta, J. L., Diez del Corral, R., de la Calle-Mustienes, E., Ferre-Marco, D. & Modolell, J. *araucan* and *caupolican*, two members of the novel iroquois complex, encode homeoproteins that control proneural and vein-forming genes. *Cell* **85,** 95–105 (1996).
21. Wheeler, S. R., Carrico, M. L., Wilson, B. A., Brown, S. J. & Skeath, J. B. The expression and function of the *achaete-scute* genes in *Tribolium castaneum* reveals conservation and variation in neural pattern formation and cell fate specification. *Development* **130,** 4373–4381 (2003).
22. Campuzano, S. *et al.* Molecular genetics of the *achaete-scute* gene complex of *D. melanogaster*. *Cell* **40,** 327–338 (1985).
23. Sturtevant, M. A., Biehs, B., Marin, E. & Bier, E. The *spalt* gene links the A/P compartment boundary to a linear adult structure in the *Drosophila* wing. *Development* **124,** 21–32 (1997).
24. de Celis, J. F. & Barrio, R. Function of the *spalt/spalt-related* gene complex in positioning the veins in the *Drosophila* wing. *Mech. Dev.* **91,** 31–41 (2000).
25. Abouheif, E. & Wray, G. A. Evolution of the gene network underlying wing polyphenism in ants. *Science* **297,** 249–252 (2002).
26. Beeman, R. W., Brown, S. J., Stuart, J. J. & Denell, R. E. in *Molecular Insect Science* (eds Hagedorn, H. H., Hildebrannd, J. G., Kidwell, M. G. & Law, J. H.) 21–29 (Plenum, New York, 1990).
27. Beeman, R. W. & Stauth, D. M. Rapid cloning of insect transposon insertion junctions using 'universal' PCR. *Insect Mol. Biol.* **6,** 83–88 (1997).
28. Quennedey, A. & Quennedey, B. Morphogenesis of the wing anlagen in the mealworm beetle *Tenebrio molitor* during the last larval instar. *Tissue Cell* **22,** 721–740 (1990).

Supplementary Information accompanies the paper on **www.nature.com/nature**.

Acknowledgements We thank G. Bucher, M. Weber and M. Klingler for the *pu11* enhancer-trap line, R. White for the FP6.86 antibody, DSHB for the 4D9 antibody and G. Pflugfelder for sharing information about *omb* degenerate primers. We thank K. Leonard for maintaining beetle stocks, T. Shippy for discussion and reading and S. Brown, R. Beeman, S. Haas and all the Manhattan beetle/insect laboratory members for discussion and comments. Y.T. thanks A. Sato and T. Yamaguchi for discussion. This work was supported by the international Human Frontier Science Program Organization (Long-term Fellow) and the National Science Foundation.

Competing interests statement The authors declare that they have no competing financial interests.

Correspondence and requests for materials should be addressed to Y.T. (tomoyasu@ksu.edu). The sequences are available in GenBank under the following accession numbers. *Tc-sal*: AY600513; *Tc-iro*: AY600514; *Tc-omb*: AY600516.

Postnatal isl1$^+$ cardioblasts enter fully differentiated cardiomyocyte lineages

Karl-Ludwig Laugwitz[1]*, Alessandra Moretti[1]*, Jason Lam[1]*, Peter Gruber[3], Yinhong Chen[1], Sarah Woodard[1], Li-Zhu Lin[1], Chen-Leng Cai[1], Min Min Lu[4], Michael Reth[5], Oleksandr Platoshyn[2], Jason X.-J. Yuan[2], Sylvia Evans[1] & Kenneth R. Chien[1]

[1]*Institute of Molecular Medicine and* [2]*Department of Medicine, University of California, San Diego, School of Medicine, La Jolla, California 92093, USA*
[3]*Children's Hospital of Philadelphia, Cardiac Center, Philadelphia, Pennsylvania 19104, USA*
[4]*Cardiovascular Division, Department of Medicine, University of Pennsylvania, Philadelphia, Pennsylvania 19104, USA*
[5]*Max-Planck Institut für Immunbiologie, Universität Freiburg, Biologie III, Abteilung Molekulare Immunologie, Freiburg 79108, Germany*

* These authors contributed equally to this work

The purification, renewal and differentiation of native cardiac progenitors would form a mechanistic underpinning for unravelling steps for cardiac cell lineage formation, and their links to forms of congenital and adult cardiac diseases[1–3]. Until now there has been little evidence for native cardiac precursor cells in the postnatal heart[4]. Herein, we report the identification of isl1$^+$ cardiac progenitors in postnatal rat, mouse and human myocardium. A cardiac mesenchymal feeder layer allows renewal of the isolated progenitor cells with maintenance of their capability to adopt a fully differentiated cardiomyocyte phenotype. Tamoxifen-inducible Cre/lox technology enables selective marking of this progenitor cell population including its progeny, at a defined time, and purification to relative homogeneity. Co-culture studies with neonatal myocytes indicate that isl1$^+$ cells represent authentic, endogenous cardiac progenitors (cardioblasts) that display highly efficient conversion to a mature cardiac phenotype with stable expression of myocytic markers (25%) in the absence of cell fusion, intact Ca^{2+}-cycling, and the generation of action potentials. The discovery of native cardioblasts represents a genetically based system to identify steps in cardiac cell lineage formation and maturation in development and disease.

In skeletal muscle, satellite cells are considered specialized endogenous muscle precursors (that is, myoblasts) that are pre-programmed to enter the skeletal muscle lineage[5,6]. Despite intensive inquiry, there has been no clear evidence for a native cardiac progenitor population with similar characteristics in the myocardium. Various cell surface markers have been used to purify precursor cells from heart muscle including c-kit and sca-1 (refs 7, 8), but the precise role of these cells in *in vivo* cardiogenesis is unclear and the efficiency of conversion to fully differentiated myocytes, in the absence of fusion, is relatively low[9–11]. Taking advantage of a developmental lineage marker for undifferentiated cardiogenic precursor cells as a requirement for a heart-specific origin, we have identified in the postnatal heart a novel cardiac cell type. The LIM-homeodomain transcription factor islet-1 (isl1) marks a cell population that makes a substantial contribution to the embryonic heart, comprising most cells in the right ventricle, both atria, the outflow tract and also specific regions of the left ventricle[12].

A subset of isl1$^+$ undifferentiated precursors remains embedded in the embryonic mouse heart after its formation and their number decreases progressively from embryonic day 12.5 (ED12.5) to ED18.5 (Fig. 1a–d). After birth, relatively few isl1$^+$ cardioblasts were still detectable, averaging 500 to 600 in the myocardium of a 1–5-day-old rat (Fig. 1e, f). Their organ distribution matched the defined contributions of isl1$^+$ embryonic precursors (Fig. 1i), suggesting these cells are developmental remnants of the fetal progenitor population. Clusters of isl1$^+$ cardioblasts were observed in both atria, whereas in the ventricles they occurred mostly as single cells (Fig. 1e, f). The localization of isl1$^+$ progenitors in specific cardiac segments (atrial muscle wall, intra-atrial septum, conus muscle, right ventricle) was conserved among diverse species: mouse, rat and human (Fig. 1g, h; Supplementary Table 1).

Using conditional genetic marking techniques in the mouse, we performed Cre-recombinase-triggered cell lineage tracing experiments to irreversibly mark isl1-expressing cells as well as their differentiated progeny during embryonic development (Fig. 2). Isl1-IRES-Cre mice[13] were crossed into the conditional Cre reporter strain R26R[14], in which Cre-mediated removal of a stop sequence results in the ubiquitous expression of the lacZ gene under the control of the endogenous Rosa26 promoter (Fig. 2a). In neonatal mice bearing both alleles a high proportion of right ventricular myocardium expressed β-galactosidase (β-gal) detected by 5-bromo-4-chloro-3-indolyl-β-D-galactoside (X-gal) staining (Fig. 2a). Around 30–40% of cardiac myocytes isolated from double heterozygous hearts stained positive for X-gal and displayed co-expression of β-gal and sarcomeric α-actinin (Fig. 2b), demonstrating that a significant proportion of myocytes originate from isl1$^+$ cardiac progenitors.

To achieve temporal and spatial control of Cre expression